NeuroImage 85 (2014) 823–833

Contents lists available at ScienceDirect

NeuroImage

journal homepage: www.elsevier.com/locate/ynimg

Glutamatergic correlates of gamma-band oscillatory activity during cognition: A concurrent ER-MRS and EEG study

Níall Lally [a,b], Paul G. Mullins [b], Mark V. Roberts [b], Darren Price [b,c], Thomas Gruber [d], Corinna Haenschel [b,e,*]

[a] Institute of Cognitive Neuroscience, University College London, UK
[b] School of Psychology, Bangor University, Bangor, UK
[c] Sir Peter Mansfield Magnetic Resonance Centre, University of Nottingham, Nottingham, UK
[d] Institute of Psychology, Osnabrück University, Germany
[e] School of Psychology, City University, London, UK

ARTICLE INFO

Article history:
Accepted 18 July 2013
Available online 25 July 2013

Keywords:
Glutamate
Functional MRS
Evoked gamma-band oscillatory activity
Repetition-priming
Repetition suppression
Repetition-enhancement

ABSTRACT

Frequency specific synchronisation of neuronal firing within the gamma-band (30–70 Hz) appears to be a fundamental correlate of both basic sensory and higher cognitive processing. In-vitro studies suggest that the neurochemical basis of gamma-band oscillatory activity is based on interactions between excitatory (i.e. glutamate) and inhibitory (i.e. GABA) neurotransmitter concentrations. However, the nature of the relationship between excitatory neurotransmitter concentration and changes in gamma band activity in humans remains undetermined. Here, we examine the links between dynamic glutamate concentration and the formation of functional gamma-band oscillatory networks. Using concurrently acquired event-related magnetic resonance spectroscopy and electroencephalography, during a repetition-priming paradigm, we demonstrate an interaction between stimulus type (object vs. abstract pictures) and repetition in evoked gamma-band oscillatory activity, and find that glutamate levels within the lateral occipital cortex, differ in response to these distinct stimulus categories. Importantly, we show that dynamic glutamate levels are related to the amplitude of stimulus evoked gamma-band (but not to beta, alpha or theta or ERP) activity. These results highlight the specific connection between excitatory neurotransmitter concentration and amplitude of oscillatory response, providing a novel insight into the relationship between the neurochemical and neurophysiological processes underlying cognition.

Introduction

Converging evidence from multiple neuroscience disciplines indicates that frequency-specific temporal synchronisation of neuronal firing is critical for the co-ordination of neuronal network assemblies underlying both basic sensory and motor processing (Singer, 1999; Womelsdorf et al., 2006) as well as a variety of cognitive functions (for a recent review see for instance:Herrmann et al., 2010; Jensen et al., 2007). In both humans and animals, synchronisation in the gamma-band frequency (30–70 Hz) is considered to play an important role in local cortical information processing (Fries, 2009).

Gamma-band oscillatory activity can typically be observed as an early evoked and a later induced response (Tallon-Baudry and Bertrand, 1999). Evoked oscillatory activity is tightly time-locked to stimulus-onset and typically occurs less than 250 ms after stimulus onset. Evoked gamma-band activity is modulated by physical stimulus properties and there is increasing evidence showing evoked gamma-band oscillatory modulation also by higher cognitive processes, like memory, attention and context processing (Busch et al., 2008; Debener et al., 2003; Fründ et al., 2008; Haenschel et al., 2000; Herrmann et al., 2004; Oppermann et al., 2012; Roye et al., 2010). The induced gamma-band response occurs after a variable time lag across trials, and reflects the subsequent processing stages within cortical networks (Hassler et al., 2011; Martinovic and Busch, 2011). Both evoked and induced gamma band activity have been linked to in-vitro measured local field potential gamma-band oscillatory activity (Haenschel et al., 2000; Hall et al., 2005; Ronnqvist et al., 2013).

As the importance of gamma-band oscillatory activity has become increasingly appreciated (e.g. Fries, 2009) a considerable effort has been made to reveal the neural mechanisms for its generation. In-vitro studies of changes in neuronal assembly activity in response to specific pharmacological agents indicate that gamma-band activity

Abbreviations: ER-MRS, Event-related magnetic resonance spectroscopy; ^{1}H-MRS, Proton magnetic resonance spectroscopy; fMRS, Functional magnetic resonance spectroscopy; EEG, electroencephalography; LOC, Lateral occipital cortex; AMPA, α-amino-3-hydroxy-5-methyl-4-isoxazolepropionic acid; NMDA, N-methyl-D-aspartate; GABA, gamma-aminobutyric acid; FID, Free induction decay.

* Corresponding author at: School of Psychology, City University, Northampton Square, London EC1V 0HB, UK. Fax: +44 207040 8580.
E-mail address: corinna.haenschel.1@city.ac.uk (C. Haenschel).

http://dx.doi.org/10.1016/j.neuroimage.2013.07.049
1053-8119/

can be generated by local networks of chemically and electrically coupled inhibitory gamma-aminobutyric acid (GABA)-ergic interneurons, and controlled by excitatory glutamatergic receptor activation (Fuchs et al., 2007; Whittington et al., 1995). More specifically, gamma oscillations can be elicited by tonic activation of ionotropic glutamate kainate, as well as cholinergic receptors (Buhl et al., 1998; Cunningham et al., 2003; Rodriguez et al., 2004; Wespatat et al., 2004), and transiently by activation of ionotropic (α-amino-3-hydroxy-5-methyl-4-isoxazolepropionic acid; AMPA, N-methyl-D-aspartate; NMDA) or metabotropic glutamate receptors. Combining both in-vitro and in-vivo techniques, research in animal models confirms that the balance between excitation and inhibition modulates the gamma-band oscillatory frequency (Atallah and Scanziani, 2009).

The links between gamma-band activity and changes in neurotransmitter concentrations within humans remain largely unknown. Fortunately, proton magnetic resonance spectroscopy (^{1}H-MRS) allows in-vivo measurement of neurotransmitter concentrations (such as GABA and glutamate) in humans, and can be combined with neurophysiological measures of oscillatory activity. A recent study measured *resting-state* GABA concentration in the visual cortex across individuals and correlated these levels with subsequent measures of peak induced gamma-band oscillatory frequency during a simple visual task measured with magnetoencephalography (Muthukumaraswamy et al., 2009). However, static measures of neurotransmitter concentration during a resting-state period may ignore critical changes in concentrations that occur during task performance. Furthermore, a direct relationship between glutamate levels and gamma-band activity, in either peak frequency or power, has not been demonstrated.

^{1}H-MRS is well established to provide reliable static resting-state measures of glutamate concentration, with several optimal acquisition schemes being suggested (Hancu, 2009; Henry et al., 2011; Jensen et al., 2009; Mayer and Spielman, 2005; Mullins et al., 2008; Schubert et al., 2004). Recently, functional changes in glutamate levels due to experimental manipulation have also been reported (Mangia et al., 2007; Mullins et al., 2005). Nonetheless, the abovementioned ^{1}H-MRS experiments used long blocks of repetitive stimulation (5+ minutes), potentially causing glutamatergic response attenuation through stimulus adaptation. Surmounting this limitation, Gussew et al. (2010) instead acquired time-locked spectral measures of glutamate levels post-stimulus onset (in response to pain). Here, we wish to develop this method further by acquiring event-related ^{1}H-MRS (ER-MRS) measures of glutamate levels during a cognitive task, in a similar vein to event-related fMRI designs, while also simultaneously collecting EEG.

Glutamate, the primary excitatory neurotransmitter, is released by approximately 80% of synapses (Magistretti et al., 1999) and is considered to play a fundamental role in learning and memory. Presynaptic glutamate release activates three different glutamate gated ion channels on postsynaptic membranes: NMDA, AMPA and kainate receptors. Both AMPA and NMDA receptor activity have been shown to jointly modulate learning and memory, whereas the role of kainate receptors in synaptic plasticity is less well understood. AMPA receptors are more common and mediate fast excitation, whereas NMDA receptors generate a much slower and longer-lasting current, and, in addition are important for Ca^{2+}-dependent plasticity. The classical view is that AMPA receptors affect short-term changes in synaptic strength; whereas NMDA receptors regulate genes that are required for the long-term maintenance of these changes (Myme et al., 2003; Rao and Finkbeiner, 2007). Indeed, long-term potentiation, the proposed mechanism of learning and memory, can be abolished by blocking glutamatergic NMDA receptors (Bliss and Collingridge, 1993), with consequent impairment in learning and memory (Morris, 1989). However, more recent evidence suggests that both AMPA and NMDA receptors have a role in long-term plasticity (Rao and Finkbeiner, 2007). NMDA and AMPA receptors are scaled proportionally so that the ratio of currents through these channels is relatively fixed, which may help to preserve the information content of synaptic transmission or may play an important role in coupling synaptic activity to long-term modification via gene expression (Myme et al., 2003; Rao and Finkbeiner, 2007). Hence, glutamate is likely to play an important role in the formation of learning related networks.

To assess the temporal relationship between event-related modulations of glutamate concentration and gamma-band activity, we simultaneously recorded stimulus-elicited changes in both ^{1}H-MRS and electroencephalography (EEG) during a repetition-priming task. We repeatedly presented pictures of familiar objects and unfamiliar abstract stimuli, respectively. The repetition of familiar stimuli usually results in a decrease in neural activity (repetition suppression), whereas the repetition of unfamiliar stimuli is typically accompanied by an increase in neural activity (repetition enhancement; see e.g. Henson et al., 2000; Martens and Gruber, 2012). Thus, repetition-priming paradigms are especially suited to examine learning related changes within cortical networks.

We focused our analysis primarily on the early-evoked gamma responses. The reason for this approach was threefold:

(1) ^{1}H-MRS can only be measured from one voxel, hence we had to choose an area (2 cm^3) to measure changes in glutamate concentration during repetition priming. We focused on an early visual area, specifically the lateral occipital cortex (LOC), a region known to be object selective (Grill-Spector et al., 1999; Grill-Spector et al., 2001) and also localized as a source of evoked gamma-band oscillatory activity (Gruber et al., 2006).
(2) There is increasing evidence showing that evoked gamma band activity is sensitive to mnemonic functioning (see above). Specifically, evoked gamma band activity has been shown to be larger for objects compared to abstract stimuli during speeded responses (Fründ et al., 2008; Herrmann et al., 2004) and to exhibit repetition suppression in some participants with a strong behavioural repetition-priming effect again when instructed to respond as quickly as possible (Busch et al., 2008). The prompt appearance of evoked gamma-band activity highlights that it is an especially good index of rapid mental processes, such as the fast processing of incoming information (Busch et al., 2008; Fründ et al., 2008; Oppermann et al., 2012).
(3) The quantification of induced, but not evoked, gamma-band oscillatory activity using EEG remains controversial due to the potentially confounding signal interference caused by miniature eye movements (Yuval-Greenberg et al., 2008). Even though there are published algorithms that can deal with such artefacts (Hassler et al., 2011), it remains an open question how to deal with these artefacts when recoding EEG data inside the MRI scanner. This is because the removal of miniature saccade-related and MRI-related artefacts is both based on independent component analysis (ICA). If ICA is applied twice and an artefact-related component is pruned in the first run of the ICA, the prerequisites for the second run of ICA (namely independence) cannot thereafter be guaranteed.

For these reasons, we chose to instruct participants to respond as quickly and accurately as possible and to focus our analysis primarily on the early-evoked responses (especially in the gamma-band, but we also included evoked theta, alpha and beta oscillatory activity and ERPs as control analyses for the specificity of our results).

In summary, the aim of the present study was to investigate if there was a relationship between event-related glutamate concentrations in the LOC and concurrently acquired task-specific evoked gamma-band oscillatory activity during early mnemonic processing.

Materials and methods

Participants

Fourteen healthy right-handed participants (8 males; M = 23.79 years, SD = 3.9) were recruited via advertisements on the Bangor

University Psychology research participation forum. Participants reported no history of neurological disorder, had normal or corrected-to-normal vision and were financially remunerated for their time. Informed consent was obtained from all participants and the study was approved by the ethics committee of the School of Psychology at Bangor University, United Kingdom.

Experimental paradigm

The behavioural task has been described in detail elsewhere (Gruber and Müller, 2005). In brief, participants categorised sequentially presented line drawings as either object or abstract stimuli (scrambled versions of unpresented objects; Fig. 1A). The stimulus set comprised of 256 unique randomly selected stimuli, 128 familiar objects and 128 abstract forms. Each stimulus was repeated three times with between one-to-four (randomised) intervening items, thus engaging processes of visual repetition priming. Categorisation was performed via (counterbalanced) button press. Participants were instructed to respond as quickly and accurately as possible. Each trial consisted of a 1850–2050 ms baseline period during which a fixation cross was shown, followed by presentation of a stimulus picture for 700 ms. The stimulus was then replaced by the fixation cross which remained onscreen for 250–450 ms, such that each individual trial was 3 s in length. There were 768 trials in total, which were spread across three same-session runs. The task was presented using E-Prime 2.0 software (Psychology Software Tools, Pittsburgh, PA).

EEG

EEG was recorded continuously at 5 kHz using a compatible EEG BrainAmp MR system (BrainProducts, Munich, Germany) and an MRI compatible BrainCap electrode cap (Falk Minow Services, Herrsching-Breitbrunn, Germany) containing 64 sintered Ag/AgCl electrodes. Each subject's heartbeat was measured using two bipolar electrocardiogram (ECG) electrodes placed approximately on the mid-clavicle line around the third intercostal space of the chest and the fifth intercostal space of the back. One additional electrode was placed below the eye to record eye-movements. The impedance of each electrode was maintained below 20 kΩ. MRI acquisition was synced to the BrainAmp MR system using a SyncBox (Brain Products). For the analysis, a low pass filter was set to 250 Hz and the electrodes were referenced to Cz. An ICA based on the Infomax (Bell and Sejnowski, 1995) optimization-learning algorithm was applied to correct for MRI specific artefacts (e.g. cardioballistic interference). The ICA aggregated variance associated with the ECG electrodes in a rolling averaged template, which updated (every 21 intervals of 600 ms) as it proceeded throughout the data. Subsequently, EEG data were visually inspected so that heartbeat and other artefacts (muscle movement and eye blinks) could be removed. Thereafter, data were segmented into epochs from 200 ms before, to 600 ms after, stimulus onset using Brain Vision Analyser 2 (Brain Products, Munich, Germany).

Evoked oscillatory activity

Evoked gamma-band activity was analysed by Morlet wavelet analysis, as proposed by Bertrand and Pantev (1994), using custom Matlab (version 7.7; Mathworks, Natick, MA, USA) scripts, from 19 electrodes around central, parietal and occipital electrode positions (mounted at or around the following standard electrode positions: Cz-C2-CP2, CPz, Cz-C1-CP1, CP2-CP4, P2, Pz, P1, CP1-CP3, P6-CP6, P4-PO4, POz-PO4, POz-PO3, P3-PO3, P5-CP5, P8-PO8, O2, Oz, O1, P7-PO7). These electrodes were chosen based on our a priori hypothesis that evoked oscillatory gamma-band activity, our focus here, would be primarily localized to posterior regions, as they were with previous use of this task (Gruber and Müller, 2005) and because of our aim to correlate evoked gamma activity with glutamate concentration measured at LOC. This Morlet wavelet analysis technique permits the examination of frequency band variations across the time domain. Specifically, the evoked response was calculated per condition (stimulus type × presentation) for each subject by averaging the EEG signal across all trials. Next, the averaged signal was transformed into the time-frequency domain via convolution with the Morlet wavelet, the absolute value of this transformation was quantified and the post-stimulus-onset period was baseline corrected by the averaged 200 ms period of activity prior to stimulus-onset. Data from the different electrode channels were averaged following wavelet decomposition. In order to achieve good time and frequency resolution in the gamma frequency range the wavelet family used was defined by a constant of 7, with an analysis frequency ranging from 0.97 to 97.66 Hz in 0.49 Hz steps; statistical analysis was performed between 30 and 50 Hz. In addition, we analysed evoked theta (4–7Hz), alpha (8–12 Hz), and beta (12–30 Hz) band activity in order to examine if there was a relationship between these frequency bands and stimulus repetitions, as well as with glutamate concentration. Only correct trials were included in the analysis following artefact reduction. Because gamma-band activity was mainly distributed between 30 and 50 Hz, we determined the peak frequency by identifying the highest amplitude across task conditions for each participant within our time-frame and frequency range of interest. One participant was excluded from the oscillatory analysis and subsequent correlations because of electrical interference.

Event related potentials (ERPs)

ERP data were analysed using the Brain Vision Analyser 2 software (Brain Products, Munich, Germany). A 30 Hz low-pass filter (0.01 Hz high pass filter, with a 12 dB/oct slope) was applied to the data before the event related potential (ERP) analysis, prior to segmenting into epochs 200 ms before to 600 ms after stimulus onset. Any epoch containing residual scanner, cardioballistic, movement or eye blink artefacts, identified through visual inspection was removed. Baseline correction was applied using the pre-stimulus interval prior to averaging and re-referencing to a global average reference. Only correct trials were included in the averages. Four main ERP components, P1, N1, L1 and L2, were identified based on the topography, deflection and latency characteristics of the respective grand average ERPs time-locked to stimulus presentation. Epochs of interest for each component were defined on the basis of deflection extreme in the mean global field power (MGFP; Picton et al., 2000). Peak detection was time-locked to the electrode of maximal amplitude (nearest 10–20 equivalent site given) for each component; P1 (90–150 ms) maximal at Oz, N1 (151–190 ms) maximal at PO8, L1 (210–350 ms) maximal at P8 and L2 (360–520 ms) maximal at P8.

Peak and mean amplitudes and latencies were analysed using stimulus type (object, abstract) × repetition (1st, 2nd, 3rd) × laterality (right, left) × electrode. A cluster of three electrodes were taken around the maximal site, with a corresponding cluster in the opposite hemisphere. Greenhouse-Geisser corrections were applied to all analyses of ERP data, unless otherwise stated only significant main effects and interactions where corrected $p < .05$ are reported.

MRI

MR images and single voxel ^{1}H-MRS were acquired on a Philips 3 T Achieva MRI System (Eindhoven, Netherlands) using an 8-channel SENSE head coil. For each participant we obtained a high resolution 3D T1 weighted image covering the whole brain ($1 \times 1 \times 1$ mm voxel resolution, field of view = 240 mm, number of excitations = 1, resolution = 240×240, 150 slices, TR (repetition time) = 8.40 ms, TE (echo time) = 3.80 ms, flip angle = 8°) to allow anatomical localisation for MRS voxel placement. Time-locked spectra, between 950 and 1150 ms after each stimulus presentation, were acquired in all subjects using a single voxel PRESS acquisition ($20 \times 20 \times 20$ mm, TR = 3000 ms, TE = 40 ms) in the lateral occipital cortex (LOC), an area of the visual cortex shown to preferentially respond to objects compared

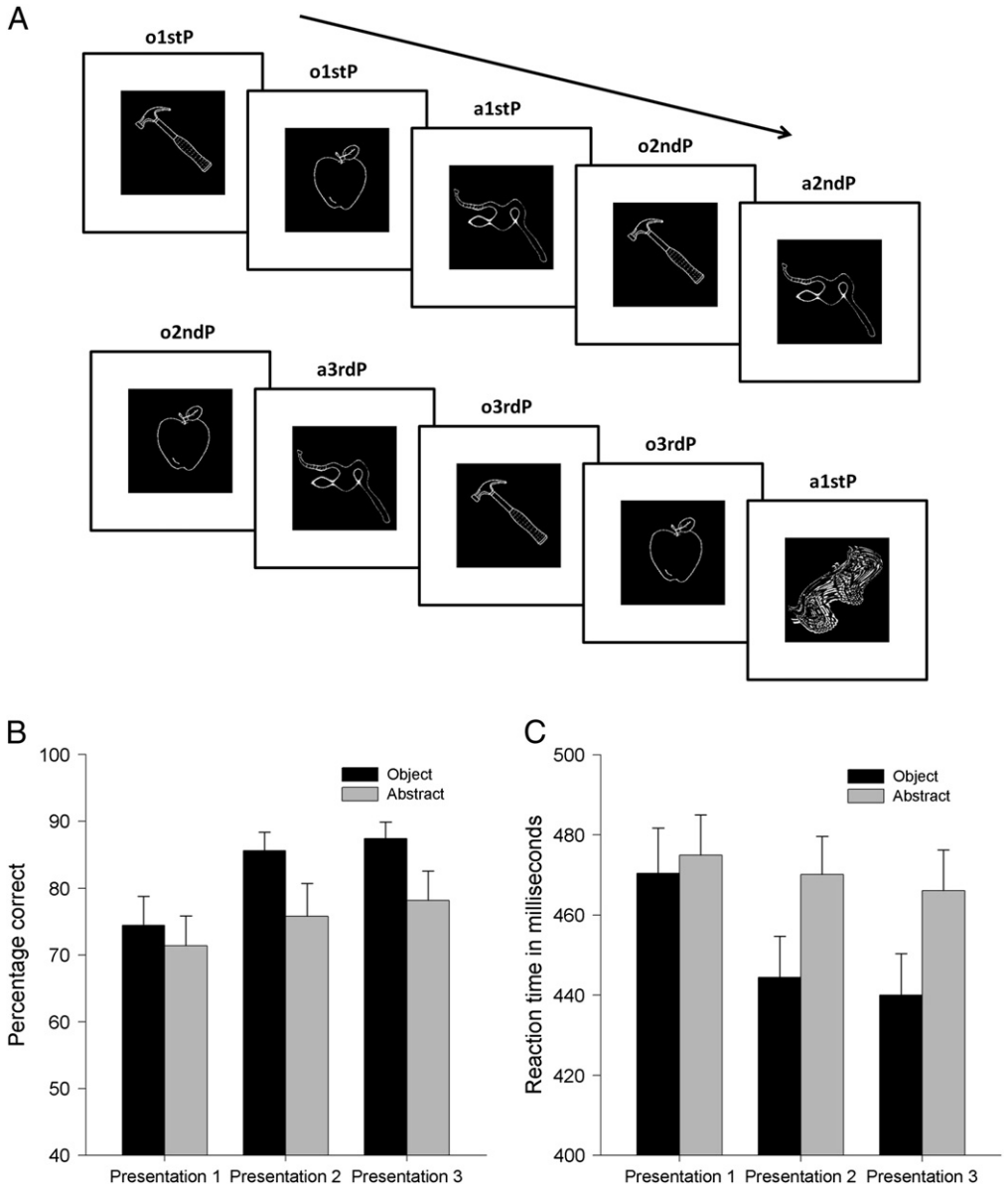

Fig. 1. Repetition priming task and behavioural results. (A) Example of object (o) and abstract (a) stimuli presented for the first (1stP), second (2ndP) and third (3rdP) time. Stimuli repeated between one and four intervening stimuli following initial presentation. (B) Percentage correct and (C) reaction time in milliseconds for object (black) and abstract (grey) stimuli across three presentations. Error bars represent SE.

to other stimuli (Grill-Spector et al., 2001) and also a localized region of evoked gamma-band oscillatory activity with this task (Gruber et al., 2006). The LOC was located using anatomical landmarks and confirmed with a blood-oxygen-level-dependent functional magnetic resonance imaging localizer (TR = 2000 ms, TE = 40 ms) in one subject using a block design (Fig. 4A). A PRESS ^{1}H-MRS sequence with a TE of 40 ms was chosen as this combination has previously been shown to provide reliable measures of glutamate at 3 T by reducing the overlapping signals from glutamine that previously hampered separation of these two metabolites (Hancu, 2009; Hancu and Port, 2011; Mullins et al., 2008). Shim settings were manually optimized for each participant to achieve full-width half maximum <12 Hz. Higher order shims were used for all cases.

As the use of an ER-MRS acquisition has only been reported twice before (Gussew et al., 2010; Nishitani, 2003), further explanation of ^{1}H-MRS acquisition in an event related paradigm with particular consideration of temporal specificity is warranted. For each experimental trial (N = 768) of the repetition priming paradigm, one ^{1}H-MRS measurement occurred. Each individual ^{1}H-MRS acquisition involved excitation by a train of radiofrequency pulses centered on the main resonance frequency of tissue water in the voxel of interest, followed by the collection of signal from the tissue 40 ms after excitation. This signal is a decaying waveform (the free induction decay; FID) composed of frequencies corresponding to the resonance frequencies of the neurometabolites present within the voxel. A Fourier transform of this decaying waveform allows the spectrum of resonance frequencies corresponding to these metabolites to be visualized, with peak height, or signal strength being determined by chemical concentration amongst other factors (for a good summary of these factors see (Alger, 2010)). Here, the FID was acquired over 1024 ms, after Fourier transformation the spectra produced is a weighted average measure of the chemical levels across this time period, with the first points of the FID providing the majority of signal power. The ^{1}H-MRS acquisition window of 950–1150 ms post-stimulus onset in this experiment corresponds to the time window in which ^{1}H-MRS data acquisition began, and was chosen to provide a clear EEG signal without the overlapping magnetic gradient artefacts. Here, stimulus presentation was triggered from the previous ^{1}H-MRS data acquisition (synchronized with the first excitation

phase) with the individual ^{1}H-MRS spectra always separated by a repetition time of 3000 ms. To prevent possible entrainment and anticipation, the stimulus presentation was jittered, leading to the individual spectral collection starting between 950 and 1150 ms after stimulus onset. This timing means that here we are sampling the metabolic concentrations at a time point ~1 s after stimulus onset. This time point was based purely on practical concerns, aiming to provide the best chance of clean EEG data with minimal ^{1}H-MRS gradient artefact. However, very few studies have examined glutamate related activity changes in this fashion, and it is unclear how they may relate to EEG measures. In addition, as there are no data from ^{1}H-MRS studies describing the time course of the glutamatergic response, the precise temporal profile of the glutamate response is not known. Thus, it is undetermined when the ^{1}H-MRS measured glutamatergic signal may peak and how long the signal may remain elevated following a single event. Future studies sampling at a wider spread of time points may help to address this issue. However, this technique provides a specific snapshot of a particular time point and not an average across a period of stimulus presentation, which is one advantage of the time-locked ER-MRS acquisition strategy.

MRS data analysis

Spectra from incorrect trials were removed, resulting in a 21% reduction, leaving on average 303 measurements per stimulus type. Subsequently, spectra were frequency corrected and averaged within conditions to produce a spectrum for object and abstract stimuli. Analyses were then performed using java Based Magnetic Resonance User Interface (jMRUI; (Naressi et al., 2001)) software version 4.0 (http://www.mrui.uab.es/mrui). The fast time domain quantitation option (QUEST — quantitation based on quantum estimation) within jMRUI was used for metabolite concentration estimation. To exclude potential blood-oxygen-level-dependent related effects on any concentration levels reported and possible water changes during neuronal activity, results were referenced to the creatine signal, which will have experienced the same blood-oxygen-level-dependent effects in signal as glutamate. Creatine is a reliably quantifiable metabolite using ^{1}H-MRS and despite its known role in energy metabolism within muscle it is thought to remain stable over time in healthy human neurons. Values for the creatine signal here were found to be very stable for each stimulus type presented throughout the experiment (less than 1% difference in absolute measures, $t_{(11)} = 0.279$, $p = 0.785$, $d = 0.046$). Referencing to creatine reduces the need for tissue content correction, as like glutamate, creatine is only detected from the tissue. One participant was excluded from the ^{1}H-MRS analyses and subsequent correlations due to poor signal-to-noise and shim (FWHM > 14 Hz) in the ^{1}H-MRS data. Statistical tests throughout the study were two-tailed. Correlations were made using the Pearson product–moment correlation coefficient.

Statistical analysis

Repeated measures of analysis of variances (ANOVA) were used to assess the main effect of stimulus and presentation, and their interaction, on behaviour, evoked oscillatory activity and ERPs. Where applicable Greenhouse-Geisser corrections were utilised to adjust for violations of the sphericity assumption. A paired *t*-test was used to determine the difference between abstract and object for glutamate levels across participants. The relationship between stimulus averaged evoked gamma-band oscillatory activity and glutamatergic levels was examined where a significant main effect or interaction was found. In order to examine the specificity of our results we further explored the relationship between condition averaged evoked oscillatory activity across beta, alpha and theta-band oscillatory activity and mean task glutamate levels. ERP components were correlated with glutamate concentration in cases of significant task effects only. Associations between variables were assessed in all case using Pearson product–moment correlations. All statistical analyses were performed using SPSS and are reported here two tailed.

Results

Behavioural performance

One participant was excluded from the overall analyses due to repeated failure to respond within the response time limit and thus their data are not included here. The pattern of behavioural results was comparable to previous repetition priming tasks (Gruber and Müller, 2005). Participants responded correctly on average of 79% (SD = 13.35%) of the time, but showed no difference in accuracy ($t_{(12)} = 1.26$, $p = 0.231$, $d = 0.194$) between stimulus types for the initial presentation. However, overall accuracy (Fig. 1B) was significantly higher (mean difference = 7.39%) for object than abstract stimuli ($F_{(1,12)} = 13.45$, $p = 0.003$, $\eta_p^2 = 0.529$). Finally, accuracy of both stimulus types increased with repetition ($F_{(2,24)} = 38.45$, $p < 0.001$, $\eta_p^2 = 0.762$), but there was a trend towards a larger increase in accuracy for object compared to abstract stimuli (stimulus × repetition: $F_{(2,24)} = 3.63$, $p = 0.062$, $\eta_p^2 = 0.232$). Analysis of reaction times (RTs) also revealed no difference ($t_{(12)} = 1.01$, $p = 0.333$, $d = 0.07$) between stimulus types for the initial presentation. There was however an advantage for object compared to abstract stimuli ($F_{(1,12)} = 21.43$, $p = 0.001$, $\eta_p^2 = 0.641$) and a faster response speed for both stimulus types with repetition ($F_{(2,24)} = 136.18$, $p < 0.001$, $\eta_p^2 = 0.919$; Fig. 1C). Increases in speed for repeated stimuli were significantly greater for object compared to abstract stimuli (stimulus type × repetition: $F_{(2,24)} = 51.88$, $p < 0.001$, $\eta_p^2 = 0.812$).

Evoked oscillatory activity

EEG data revealed that both object and abstract stimuli elicited evoked gamma-band activity at posterior electrodes between 50 and 250 ms post stimulus onset (illustrated in Fig. 2A for the first, second and third stimulus presentation). There was a trend towards a significant difference between stimulus types following the initial presentation ($t_{(11)} = 1.967$, $p = 0.075$, $d = 0.327$), with higher evoked gamma-band oscillator activity following object that abstract stimulus types. There was no main effect of either stimulus type ($F_{(1,11)} = 0.038$, $p = 0.848$, $\eta_p^2 = 0.003$) or presentation ($F_{(2,22)} = 0.070$, $p = 0.933$, $\eta_p^2 = 0.006$). However, evoked gamma-band oscillatory activity decreased with repeated presentations of objects, but increased for repetitions of abstract stimuli (stimulus × repetition: $F_{(2,22)} = 4.578$, $p = 0.042$, $\eta_p^2 = 0.294$; Fig. 2B).

Utilizing the same analytical approach as our gamma-band analysis (i.e. the same electrodes and a post stimulus onset time window based upon data presented in Fig. 2A), we evaluated the evoked beta (12–30 Hz, 50–200 ms), alpha (8–12 Hz, 100–300 ms) and theta (4–7 Hz, 0–400 ms) activity within our paradigm. There was no significant main effect of stimulus type ($F_{(1,11)} = 2.320$, $p = 0.156$, $\eta_p^2 = 0.174$; $F_{(1,11)} = 4.076$, $p = 0.069$, $\eta_p^2 = 0.270$), repetition ($F_{(2,22)} = 1.241$, $p = 0.309$, $\eta_p^2 = 0.101$; $F_{(2,22)} = 0.577$, $\eta_p^2 = 0.294$, $p = 0.570$, $\eta_p^2 = 0.050$) or interaction (stimulus type × repetition: $F_{(2,22)} = .0.045$, $p = 0.956$, $\eta_p^2 = 0.004$; $F_{(2,22)} = 0.156$, $p = 0.857$, $\eta_p^2 = 0.014$) on beta or alpha, respectively. There was a main effect of stimulus type ($F_{(1,11)} = 7.393$, $p = 0.020$, $\eta_p^2 = 0.402$) for theta activity but none for repetition ($F_{(2,22)} = 0.193$, $p = 0.826$, $\eta_p^2 = 0.017$) nor an interaction between these two variables ($F_{(2,22)} = 0.132$, $p = 0.877$, $\eta_p 2 = 0.012$). Of note, the abovementioned trend toward a significant effect of stimulus type in the beta-band frequency analysis reflects higher average activity to objects than abstract stimuli across presentations, while the opposite pattern is true for the main effect of stimulus type in the theta-band analysis.

ERPs

We found no significant effect for the P1 amplitude. N1 amplitude was larger on the left compared to the right side ($F_{(1,12)} = 7.052$, $p = 0.002$, $\eta_p^2 = 0.352$), but showed no other significant effects. The late component L1 amplitude however was larger for abstract compared to object stimuli (stimulus type ($F_{(1,12)} = 28.08$, $p < 0.001$, $\eta_p^2 = 0.684$); see Fig. 3) and larger on the right side (laterality ($F_{(1,12)} = 7.814$, $p = 0.015$, $\eta_p^2 = 0.375$)). There was no significant difference between first or repeated repetitions of the stimulus. The late component L2 was again larger on the right side (laterality $F_{(1,12)} = 7.515$, $p = 0.017$, $\eta_p^2 = 0.366$) with no other significant main effect. There were no significant effects on latency.

^{1}H-MRS glutamate concentrations

For the analysis of glutamate, spectra were averaged separately for object and abstract stimuli across stimulus presentations (one-to-three). This produced spectra with sufficient signal to noise to reliably detect glutamate in all conditions for all participants except one. ^{1}H-MRS data quality is often determined from the Cramer Rao lower bound (CRLB) of the data, which is essentially a ratio of the standard deviation of the residual signal after modelling to the amplitude of the fitted peak. All glutamate measures used in our statistical analysis had a CRLB of <15%, which is considered a reliable cut off for ^{1}H-MRS data, and below the common exclusion criteria of CRLB 20%. ^{1}H-MRS data showed that average LOC (Figs. 4B,C) glutamate was lower following the presentation of object (M = .5222, SD = .145) than abstract (M = .5822, SD = .128) stimuli ($F_{(1,11)} = 8.06$, $p = 0.016$, $d = 0.47$; Figs. 4B, C). This result also demonstrates that ER-MRS can discriminate between these stimulus types and that variation in glutamate concentrations can potentially distinguish between different conditions in a task.

The reliability of the MRS signal is largely dependent upon the signal-to-noise ratio, which increases with the number of FIDs used to create an average spectrum. This has an adverse effect on the power of any analysis that subdivides spectra per condition. Nevertheless, consistent with our behavioural and EEG results, we also undertook an exploratory analysis to assess if a similar stimulus type effect was also visible across the three presentations, despite the substantial reduction in the number of spectral averages. Tentative (uncorrected) paired t-tests revealed a trend towards stimulus type differentiation at the third presentation, with abstract stimuli eliciting higher glutamate levels than object stimuli ($t_{(11)} = 1.92$, $p = 0.08$, $d = 0.32$). No trends for stimulus type differentiation were observed for either the first or second presentation (both $t_{(11)} < 1$). These results support our findings of glutamatergic differentiation between stimulus types (object vs. abstract), but remain tenuous due to the aforementioned reduction in signal reliability and statistical power.

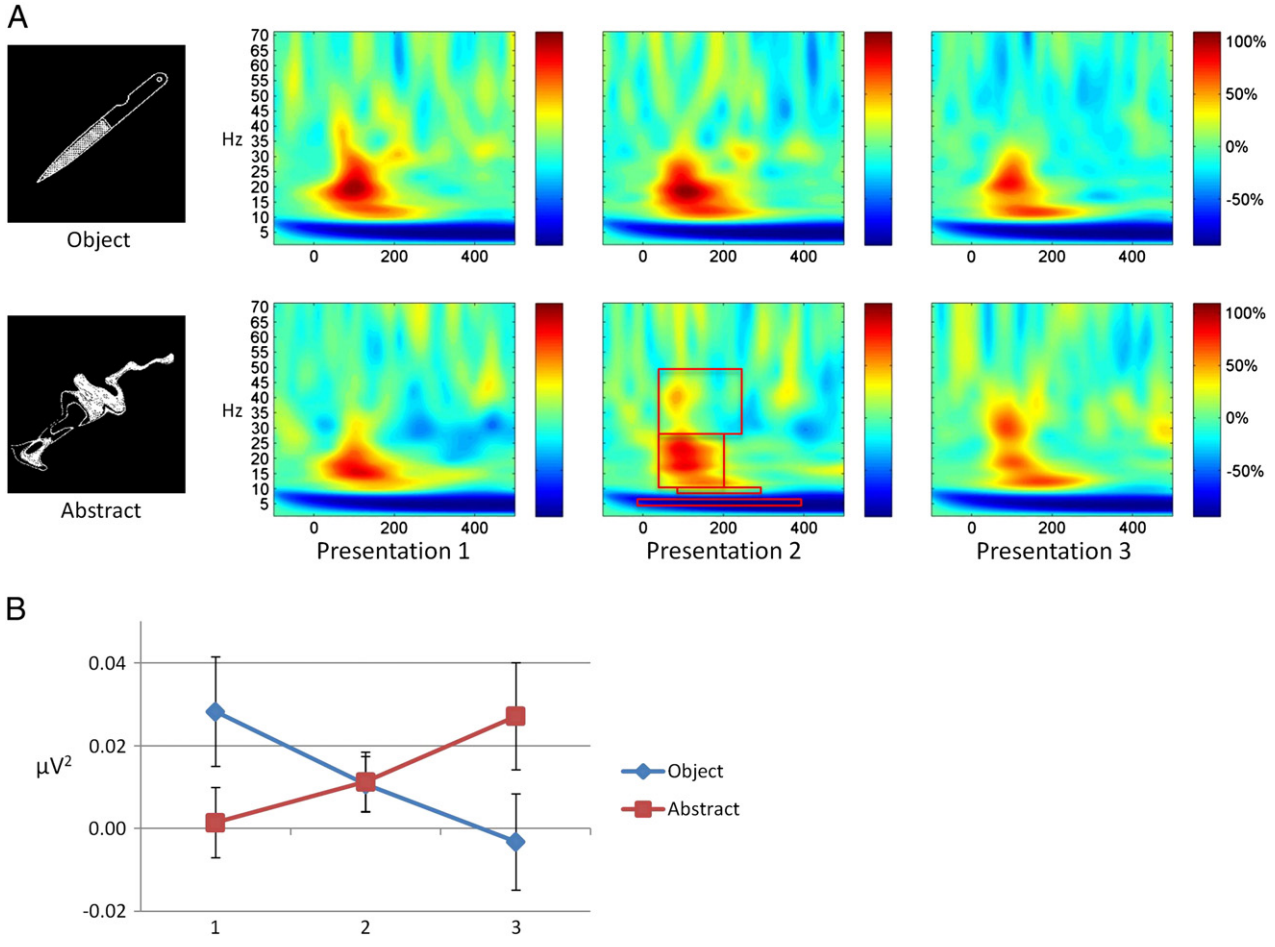

Fig. 2. Stimulus-evoked gamma-band activity. (A) Evoked oscillatory activity between 1 and 70 Hz after the first (left), second (centre) and third (right) stimulus presentation is shown for object (top row) and for abstract (bottom row) stimuli at posterior electrodes. Power is calculated as the change from baseline (−200 ms to 0 ms). Red boxes (abstract stimuli presentation 2) indicate the frequency range and time window that were quantified and analysed for gamma (30–50 Hz; 50–250 ms), beta (12–30 Hz; 50–200 ms), alpha (8–12 Hz; 100–300 ms) and theta (4–7 Hz; 0–400 ms) ranges. Note that although the evoked gamma-band power appears to be a tail of a lower frequency, this smearing commonly arises as a function of averaging across participants for the presentation of results from evoked oscillatory analyses (Fründ et al., 2008; Oppermann et al., 2012). Single subjects do not contain this visual artefact (please see S1). (B) Mean evoked gamma-band power in response to stimulus 1, 2 and 3 are shown for object (blue) and abstract (red) stimuli. We find a significant interaction between stimulus and presentation for oscillatory activity in the gamma-band (30–50 Hz; $F_{(2,22)} = 4.578$, $p = 0.042$). Error bars represent SE.

Glutamatergic correlates of gamma-band oscillatory activity

Importantly, examining the relationship between neurochemical and neurophysiological measures, we found a significant correlation between condition averaged (object and abstract combined) evoked gamma-band oscillatory power and mean glutamate levels ($r_{(11)} = .769$, $p = 0.006$; see Fig. 4D). This strong correlation reflected a positive relationship between both object ($r_{(11)} = .696$) and abstract ($r_{(11)} = .682$) glutamate levels and their respective stimulus specific mean gamma-band oscillatory evoked power. In order to ascertain the specificity of our association we assessed the relationship between baseline gamma levels (200 ms prior to stimulus onset) and mean glutamate levels. There was no significant correlation between baseline gamma oscillatory activity and glutamate levels ($r_{(11)} = .231$, $p = 0.495$). Furthermore, to assess whether the correlation coefficient between mean baseline and task gamma-band oscillatory power and glutamate concentrations was significantly different we computed Steiger's Z-test (two-tailed). We found a significant difference between the two relationships ($Z_{(8)} = 2.12$, $p = 0.0388$), indicating that relative to the baseline period, the stimulus period was associated with a significant increase in gamma-band oscillatory power that was specifically associated with average glutamate levels after the stimulus.

Moreover, we found no significant relationships between condition averaged beta ($r_{(11)} = .075$, $p = 0.826$;), alpha ($r_{(11)} = -.135$, $p = 0.691$) or theta ($r_{(11)} = -.284$, $p = 0.397$) band oscillatory power, and glutamate levels, respectively. Additionally, stimulus averaged ERP amplitude for the area under the L1 was not associated with stimulus averaged glutamate concentrations ($r_{(12)} = .258$, $p = 0.418$). Thus, we conclude that glutamate concentration is uniquely associated with the amplitude of dynamic stimulus-related gamma-band oscillatory activity.

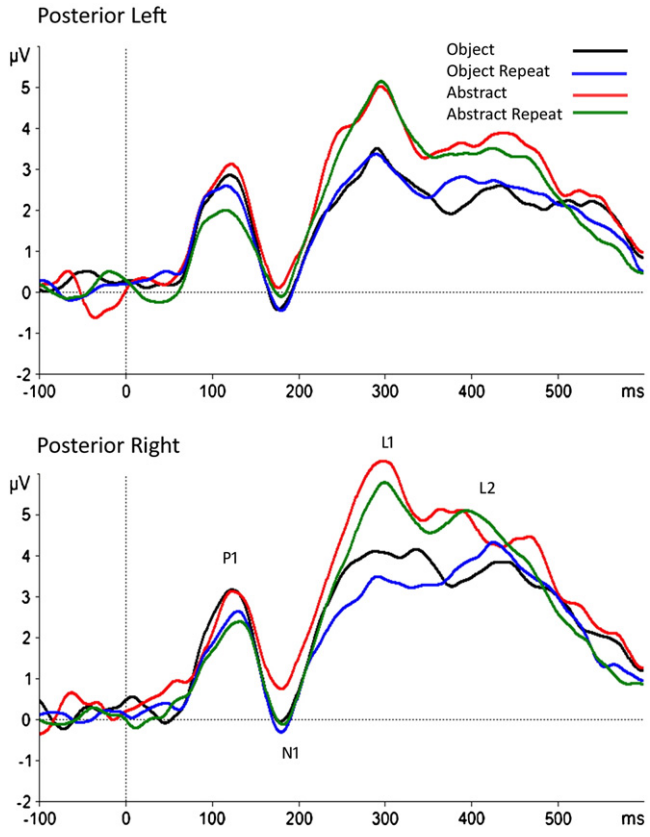

Fig. 3. Event-related potentials across stimulus type. ERPs for the left/right posterior regional means for initial presentation, and the 2nd and 3rd presentation averaged together, for object and abstract stimuli, respectively. P1, N1, L1 and L2 components are visible. A significant effect of stimulus type is apparent at L1 ($F_{(1,12)} = 28.08$, $p < 0.001$).

Finally, we investigated whether glutamate concentrations across individuals correlated with the peak gamma-band frequency (i.e. specific frequency with the highest power), which has been previously shown to be associated with baseline GABA concentration (Muthukumaraswamy et al., 2009). A trend towards a significant correlation with peak gamma-band oscillatory frequency was found ($M = 34.25$ Hz, $r_{(11)} = -.538$, $p = 0.088$), with higher glutamate levels in the LOC associated with a lower peak frequency. No significant association between LOC glutamate concentration and peak frequency was found for either beta ($r_{(11)} = .077$, $p = 0.823$), alpha ($r_{(11)} = .061$, $p = 0.858$) or theta ($r_{(11)} = .307$, $p = 0.358$) band analyses.

Discussion

Our study provides in-vivo evidence of a relationship between dynamic glutamatergic concentrations and synchronised neuronal oscillations within the gamma-frequency range during a cognitive task in the human brain. We show, using a unique combination of ER-MRS and EEG, that levels of excitatory neurotransmitter glutamate correlate significantly with the power of neuronal oscillations within the gamma-band. Specifically, we find a relationship between levels of glutamatergic activity in the LOC and stimulus evoked gamma-band amplitude during an object repetition-priming task.

Our results highlight that stimulus evoked gamma-band oscillatory power is related to glutamatergic concentration in the human brain, and thus provide complementary evidence to previous animal work assessing the underlying neurobiology of gamma-band oscillatory activity both in-vivo and in-vitro (Atallah and Scanziani, 2009; Whittington et al., 1995). Additionally, our findings add to recent research assessing the contribution of resting-state GABA levels to the peak inter-individual frequency, but not power, of the induced gamma signal (Muthukumaraswamy et al., 2009). Here, we find that dynamic glutamatergic activity levels are associated with specific stimulus-related changes in gamma power, and as a trend to peak evoked gamma-band oscillatory frequency. These results are consistent with the proposal that precise temporal tuning (frequency) of activity being determined by the ratio of GABA and glutamate concentrations (Atallah and Scanziani, 2009), while the gain of this neural signal (power) is regulated by modulations in glutamate levels only. Taken together, our findings suggest both a unique and potentially complementary role for glutamate levels in modulating gamma-band cortical networks in the human brain. Indeed, glutamate may possess a distinct role in driving gamma-oscillatory power; meanwhile, both GABA and glutamate might jointly modulate the peak gamma-band oscillatory frequency, reflecting recent in-vitro research (Atallah and Scanziani, 2009).

However, the association between glutamate concentration and oscillatory network changes here is limited to the region of ^{1}H-MRS acquisition, the LOC. Without data from other areas, generalisation to the rest of the cortex is not possible. Importantly, our results do not exclude glutamate changes in other regions of the visual cortex; future studies geared to investigate the generalizability of these relationships would be beneficial. Indeed, in contrast to our association between stimulus-related glutamate levels and evoked oscillatory activity in the gamma-range, Gallinat et al. (2006) reported a relationship between baseline hippocampal glutamate concentration and frontal theta oscillations using an auditory target detection paradigm. This suggests that the relationship between measures of synchronised oscillatory activity and glutamate concentration may be task specific. It would be interesting to investigate if the correlation between theta oscillations and glutamate concentration would still be evident if recorded simultaneously. Furthermore, despite demonstrating that our glutamatergic concentration in the LOC and gamma-band oscillatory power correlation was specific to the stimulus, but not the baseline period, this association does not preclude the possibility that other tasks and stimuli or passive viewing of the same stimuli without a task may elicit a similar

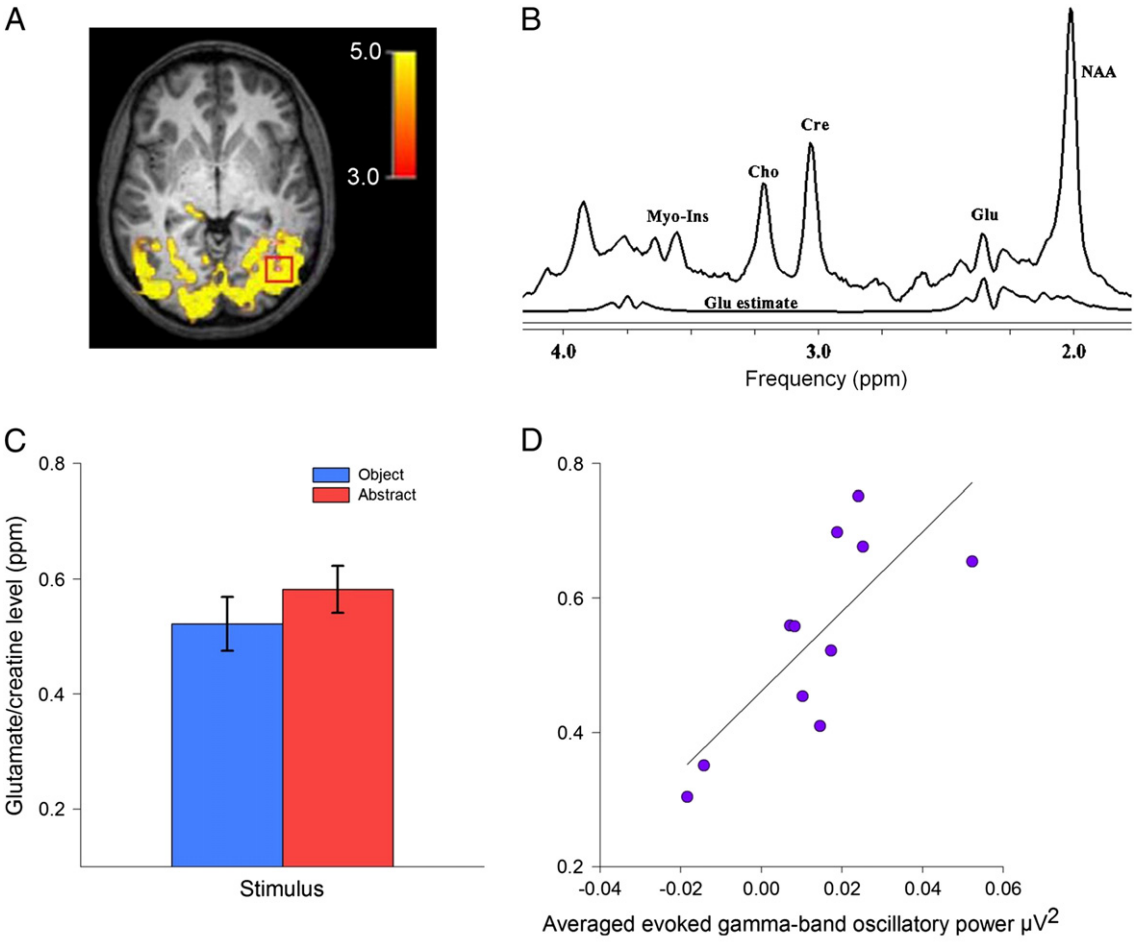

Fig. 4. ^{1}H-MRS and glutamate correlations with evoked gamma-band power. (A) The LOC (red box) was located using anatomical landmarks, and confirmed by a functional magnetic resonance imaging localizer contrasting object vs. abstract stimuli. Activity maps (red/yellow) show t-statistics. (B) Representative averaged magnetic resonance spectrum (across 384 spectra) acquired in response to presentation of one stimulus type. Spectra quality permitted the estimation of glutamate and creatine (Cre) concentration for each stimulus type (other estimates shown are NAA: N-acetyl-aspartate; Cho: Choline; Myo-Ins: myo-Inositol). The individual glutamate spectral estimation is shown in the line below. Glutamate levels are referenced to creatine, a neuronal metabolite found to be stable across conditions, to control for tissue concentration differences. (C) Glutamate levels (mM) for object (blue) and abstract (red) stimuli, showing that glutamate was significantly higher after abstract stimulus presentation ($F_{(1,11)} = 8.06$, $p = 0.016$). (D) Positive correlation ($r_{(11)} = .769$, $p = 0.006$) between mean task related gamma-band activity (μV^2) and glutamate level (mM). Error bars represent SE.

relationship. Future research is needed to clarify the specificity of the relationship evidenced here.

Repeated presentations of pictures of familiar objects resulted in a decrease of evoked gamma-band activity. These effects might be linked to a 'sharpening' mechanism within a cell assembly representing a familiar object (cf. Wiggs and Martin, 1998). In contrast, the representation of repeated abstract stimuli was associated with an increase in evoked gamma power. These findings might be a signature of the formation of a new cortical network representing an object (cf. Martens and Gruber, 2012). A similar pattern of results was reported by Gruber and Müller (2005) for the induced but not the evoked gamma-band response. A possible explanation for this contradictory finding is that memory effects can be observed in evoked and induced gamma-band oscillatory activity, but task parameters such as instructions may modulate their appearance in distinct analyses (Herrmann et al., 2010). For instance, Busch et al. (2008) and Fründ et al. (2008) showed that evoked gamma-band activity in fact is larger for objects compared to abstract stimuli and the response to object stimuli can be suppressed with repetition in cases when an immediate and speeded response is required. Indeed participants in the current study, but not the Gruber and Müller (2005) study, were instructed to respond as quickly (and accurately) as possible. Comparing RTs between the two studies directly confirmed that participants in the current study responded faster compared to the Gruber and Müller (2005) study.

Our ^{1}H-MRS results provide evidence for a significantly different glutamate response to stimulus type averaged object and abstract stimuli. Tentatively, we also investigated the mean glutamate values for each stimulus presentation, and while these means do decrease for object images, and increase for abstract images (mirroring the changes in gamma-band oscillatory power), they do not reach statistical significance. The lack of significance in the interaction between stimulus type and presentation was likely a result of decreased signal to noise ratio, and hence increased variability in the ^{1}H-MRS data averaged for each stimulus presentation. Future studies, focusing on either repetition suppression or enhancement effects, with greater acquisitions for each presentation should help to address this issue. The degree to which elevated glutamate concentrations, as measured by ^{1}H-MRS, reflect increases in either synaptic glutamate release or glutamatergic cycling as part of the energy metabolism process remains to be determined (Mullins et al., 2005). One viewpoint suggests that ^{1}H-MRS measures of glutamate differences reflect oxidative neuronal metabolism (Mangia et al., 2007), as glutamate-glutamine cycling is tightly coupled to oxidative glucose consumption (Rothman et al., 1999). However, the timescale of glutamatergic cycling is much slower (1 h for total pool turnover (Shen, 2013)) than the timescale of change in glutamate levels seen here (on the order of a second) and in other studies (Gussew et al., 2010). We therefore propose that glutamatergic synthesis cannot account for our results. The most parsimonious account for fast changes

in glutamate levels across conditions, as shown here, is neurotransmission. It is generally accepted that ^{1}H-MRS measures of neurotransmitters reflect total chemical volume within the entire tissue. However, it is unknown whether vesicular, extra synaptic or intra synaptic levels of metabolites contribute equally to the ^{1}H-MRS signal. Indeed, early work on glutamate MR visibility suggests there is a pool of ^{1}H-MRS invisible glutamate — most likely related to a subcellular neurotransmitter pool (Kauppinen et al., 1994). Therefore, we tentatively suggest that the rapid increases in ^{1}H-MRS measured neurotransmitter levels in our study, and other studies (Gussew et al., 2010), are best explained by neurotransmitter release from a ^{1}H-MRS invisible subcellular compartment to a more ^{1}H-MRS visible extracellular compartment, than by an increase in glutamate synthesis. While this interpretation of our results is speculative at present, it best fits the current data and previous studies. However, it is likely that standard ^{1}H-MRS techniques alone can never provide a definitive answer given the coarse spatial resolution of typical ^{1}H-MRS studies. Nevertheless, combining ^{1}H-MRS with other measures such as diffusion weighted spectroscopy (Valette et al., 2005) may allow us to investigate intracellular versus extra cellular changes and may provide evidence for our proposal.

In addition, with appropriate selection of varying ^{1}H-MRS data acquisition time points in future studies it might be possible to characterise the glutamatergic response in much the same way as the blood-oxygenated-level-dependent (BOLD; fMRI) response has been elucidated, which would go some way to addressing which components of glutamatergic processes are altered here. Indeed, one possible limitation of the current study is, relative to the stimulus onset, the time at which the measurement of the glutamatergic signal was acquired.

The evoked gamma-band power changes occurred between 50 and 250 ms, whereas glutamate concentration measurement started between 950 and 1150 ms post-stimulus onset. This raises the question how glutamate concentration following stimulus onset can be related to early-evoked gamma-band power. It also raises the issue how such a late measurement of glutamate concentration can be related to object recognition. One potential interpretation is that gamma-band oscillatory power drives glutamatergic activity. For example, glutamate changes in the LOC 1–2 s following stimulus onset may reflect recurrent neuronal network processes that arise from earlier oscillatory responses measured across the entire visual system. However, as the glutamatergic response profile is currently uncharted it is also possible that glutamate levels drive oscillatory activity but that the ^{1}H-MRS signal remains detectable for 1–2 s following an event. An alternative and final suggestion may be that the glutamatergic signal changes measured here in response to distinct visual stimuli mainly reflects trait but not state-dependent levels. As the ^{1}H-MRS glutamate signal is derived from total tissue glutamate concentration and only a fraction may be implicated in transmission related changes, the contribution of state-dependent changes in glutamatergic processing may primarily reflect largely stable trait processes. However, concurrent acquisition of these two measures likely increases the between measure signal-to-noise ratio and improves validity of any significant relationships that may be found. Further work is needed to characterize the profile of the glutamate signal to resolve these interpretation possibilities. Nevertheless, in all three scenarios increased glutamate in response to abstract relative to object stimuli might indicate the differential computational cost between stimulus types.

Given the recent surge in research investigating pharmacological manipulations to the glutamatergic system, particularly in the treatment of depression (Duman and Aghajanian, 2012) and schizophrenia (Egerton and Stone, 2012), the task-based event-related approach to ^{1}H-MRS demonstrated here, could provide a unique evaluation of the glutamatergic system under varied psychological conditions. The now ubiquitous BOLD contrast imaging provides an indirect measure of brain activity that can, in certain circumstances, produce misleading results. For instance, an increase in BOLD activity following acute drug administration could result as a consequence of either decreased regional blood supply or increased brain activity. Thus, the ER-MRS methodology evidenced here could provide an adjunct to BOLD imaging, which may be especially relevant to drug development protocols, therapeutic assessment and intervention research.

While we have focused in the current study on functional glutamate concentration, future research should also directly examine event-related GABA concentrations and oscillatory activity. It is likely that the balance between the excitatory glutamate and the inhibitory GABA at the level of interneurons (Mann and Mody, 2010; Whittington et al., 1995) jointly modulate synchronised oscillations, and this would be an interesting area to investigate in future ^{1}H-MRS studies. Moreover, concurrent measurements of network activity and neurochemical concentrations offer a potential opportunity to both elucidate the basis of cognition and its impairment in mental disorders. For example, schizophrenia has been proposed to result from a deficit in forming dynamic links between neuronal populations (the “disconnection” hypothesis; (Friston and Frith, 1995)), and is also linked to neurochemical dysfunction (Carlsson et al., 1999; Lisman et al., 2008; Stephan et al., 2006). There is considerable debate among theorists regarding the relative importance of glutamate and GABA dysfunctions within this disorder (Gonzalez-Burgos and Lewis, 2008; Kantrowitz and Javitt, 2012; Kegeles et al., 2012; Lewis et al., 2005). Importantly, the technique outlined here could be used to directly assess the impact of the relative importance of changes in both transmitter concentrations upon task-related changes in neural activity and performance.

Conclusions

In summary, the results provide in-vivo evidence that dynamic neural network activity during stimulus presentation is associated with glutamate levels within individuals, complementing in-vitro research. Furthermore, the present study demonstrates the feasibility of concurrently measuring stimulus and possibly cognitive task-related changes using both ^{1}H-MRS and synchronised oscillatory activity, which, exemplifies a novel neuroscientific methodology for exploring functional associations between basic biological and systems level research. We establish that simultaneously recording these measures is possible and allows critical insight into the functional relationship between neurochemical and neurophysiological processes, deepening our understanding of the underlying neurobiology of cognition.

Author contributions

C.H. conceived and C.H. and P.M. designed the experiments. C.H., N.L., M.R., D.P., P.M. performed the experiments. M.R., C.H., P.M. were responsible for the technical aspects of the combined measures. D.P. programmed the task. M.R., DP., N.L. pre-processed the EEG data. N.L., C.H., T.G. analysed the EEG data. D.P., N.L and P.M. analysed the MRS data. All were involved in the writing of the paper.

Conflict of interest

The authors declare no conflict of interest.

Acknowledgments

This work was supported by the Welsh Institute of Cognitive Neuroscience (WICN; grant WBI031) funded by the Welsh Assembly Government and the Medical Research Council. We would like to thank Alexandre Franco for the help with the Matlab code used in the analysis of the ER-MRS, and Matthew Clemence for the help with setting up the event-related ^{1}H-MRS on the Philips Scanner.

Appendix A. Supplementary data

Supplementary data to this article can be found online at http://dx.doi.org/10.1016/j.neuroimage.2013.07.049.

References

Alger, J.R., 2010. Quantitative proton magnetic resonance spectroscopy and spectroscopic imaging of the brain: a didactic review. Top. Magn. Reson. Imaging 21, 115–128.

Atallah, B.V., Scanziani, M., 2009. Instantaneous modulation of gamma oscillation frequency by balancing excitation with inhibition. Neuron 62, 566–577.

Bell, A.J., Sejnowski, T.J., 1995. An information-maximization approach to blind separation and blind deconvolution. Neural Comput. 7, 1129–1159.

Bertrand, O., Pantev, C., 1994. Stimulus frequency dependence of the transient oscillatory auditory evoked responses (40 Hz) studied by electric and magnetic recordings in human. In: Pantev, C., Elbert, T., Lutkenhoner, B. (Eds.), Oscillatory Event-Related Brain Dynamics, vol. 271. Plenum, New York, pp. 231–242.

Bliss, T.V., Collingridge, G.L., 1993. A synaptic model of memory: long-term potentiation in the hippocampus. Nature 361, 31–39.

Buhl, E.H., Tamas, G., Fisahn, A., 1998. Cholinergic activation and tonic excitation induce persistent gamma oscillations in mouse somatosensory cortex in vitro. J. Physiol. 513 (Pt 1), 117–126.

Busch, N.A., Groh-Bordin, C., Zimmer, H.D., Herrmann, C.S., 2008. Modes of memory: early electrophysiological markers of repetition suppression and recognition enhancement predict behavioral performance. Psychophysiology 45, 25–35.

Carlsson, A., Hansson, L.O., Waters, N., Carlsson, M.L., 1999. A glutamatergic deficiency model of schizophrenia. Br. J. Psychiatry 2–6 (Suppl.).

Cunningham, M.O., Davies, C.H., Buhl, E.H., Kopell, N., Whittington, M.A., 2003. Gamma oscillations induced by kainate receptor activation in the entorhinal cortex in vitro. J. Neurosci. 23, 9761–9769.

Debener, S., Herrmann, C.S., Kranczioch, C., Gembris, D., Engel, A.K., 2003. Top-down attentional processing enhances auditory evoked gamma band activity. Neuroreport 14, 683–686.

Duman, R.S., Aghajanian, G.K., 2012. Synaptic dysfunction in depression: potential therapeutic targets. Science 338, 68–72.

Egerton, A., Stone, J.M., 2012. The glutamate hypothesis of schizophrenia: neuroimaging and drug development. Curr. Pharm. Biotechnol. 13, 1500–1512.

Fries, P., 2009. Neuronal gamma-band synchronization as a fundamental process in cortical computation. Annu. Rev. Neurosci. 32, 209–224.

Friston, K.J., Frith, C.D., 1995. Schizophrenia: a disconnection syndrome? Clin. Neurosci. 3, 89–97.

Fründ, I., Busch, N.A., Schadow, J., Gruber, T., Korner, U., Herrmann, C.S., 2008. Time pressure modulates electrophysiological correlates of early visual processing. PLoS One 3, e1675.

Fuchs, E.C., Zivkovic, A.R., Cunningham, M.O., Middleton, S., Lebeau, F.E., Bannerman, D.M., Rozov, A., Whittington, M.A., Traub, R.D., Rawlins, J.N., Monyer, H., 2007. Recruitment of parvalbumin-positive interneurons determines hippocampal function and associated behavior. Neuron 53, 591–604.

Gallinat, J., Kunz, D., Senkowski, D., Kienast, T., Seifert, F., Schubert, F., Heinz, A., 2006. Hippocampal glutamate concentration predicts cerebral theta oscillations during cognitive processing. Psychopharmacology (Berl) 187, 103–111.

Gonzalez-Burgos, G., Lewis, D.A., 2008. GABA neurons and the mechanisms of network oscillations: implications for understanding cortical dysfunction in schizophrenia. Schizophr. Bull. 34, 944–961.

Grill-Spector, K., Kushnir, T., Edelman, S., Avidan, G., Itzchak, Y., Malach, R., 1999. Differential processing of objects under various viewing conditions in the human lateral occipital complex. Neuron 24, 187–203.

Grill-Spector, K., Kourtzi, Z., Kanwisher, N., 2001. The lateral occipital complex and its role in object recognition. Vision Res. 41, 1409–1422.

Gruber, T., Müller, M.M., 2005. Oscillatory brain activity dissociates between associative stimulus content in a repetition priming task in the human EEG. Cereb. Cortex 15, 109–116.

Gruber, T., Trujillo-Barreto, N.J., Giabbiconi, C.M., Valdes-Sosa, P.A., Müller, M.M., 2006. Brain electrical tomography (BET) analysis of induced gamma band responses during a simple object recognition task. Neuroimage 29, 888–900.

Gussew, A., Rzanny, R., Erdtel, M., Scholle, H.C., Kaiser, W.A., Mentzel, H.J., Reichenbach, J.R., 2010. Time-resolved functional ^{1}H MR spectroscopic detection of glutamate concentration changes in the brain during acute heat pain stimulation. Neuroimage 49, 1895–1902.

Haenschel, C., Baldeweg, T., Croft, R.J., Whittington, M., Gruzelier, J., 2000. Gamma and beta frequency oscillations in response to novel auditory stimuli: a comparison of human electroencephalogram (EEG) data with in vitro models. Proc. Natl. Acad. Sci. U. S. A. 97, 7645–7650.

Hall, S.D., Holliday, I.E., Hillebrand, A., Singh, K.D., Furlong, P.L., Hadjipapas, A., Barnes, G.R., 2005. The missing link: analogous human and primate cortical gamma oscillations. Neuroimage 26, 13–17.

Hancu, I., 2009. Optimized glutamate detection at 3 T. J. Magn. Reson. Imaging 30, 1155–1162.

Hancu, I., Port, J., 2011. The case of the missing glutamine. NMR Biomed. 24, 529–535.

Hassler, U., Barreto, N.T., Gruber, T., 2011. Induced gamma band responses in human EEG after the control of miniature saccadic artifacts. Neuroimage 57, 1411–1421.

Henry, M.E., Lauriat, T.L., Shanahan, M., Renshaw, P.F., Jensen, J.E., 2011. Accuracy and stability of measuring GABA, glutamate, and glutamine by proton magnetic resonance spectroscopy: a phantom study at 4 tesla. J. Magn. Reson. 208, 210–218.

Henson, R., Shallice, T., Dolan, R., 2000. Neuroimaging evidence for dissociable forms of repetition priming. Science 287, 1269–1272.

Herrmann, C.S., Lenz, D., Junge, S., Busch, N.A., Maess, B., 2004. Memory-matches evoke human gamma-responses. BMC Neurosci. 5, 13.

Herrmann, C.S., Fründ, I., Lenz, D., 2010. Human gamma-band activity: a review on cognitive and behavioral correlates and network models. Neurosci. Biobehav. Rev. 34, 981–992.

Jensen, O., Kaiser, J., Lachaux, J.P., 2007. Human gamma-frequency oscillations associated with attention and memory. Trends Neurosci. 30, 317–324.

Jensen, J.E., Licata, S.C., Ongur, D., Friedman, S.D., Prescot, A.P., Henry, M.E., Renshaw, P.F., 2009. Quantification of J-resolved proton spectra in two-dimensions with LCModel using GAMMA-simulated basis sets at 4 tesla. NMR Biomed. 22, 762–769.

Kantrowitz, J., Javitt, D.C., 2012. Glutamatergic transmission in schizophrenia: from basic research to clinical practice. Curr. Opin. Psychiatry 25, 96–102.

Kauppinen, R.A., Pirttila, T.R., Auriola, S.O., Williams, S.R., 1994. Compartmentation of cerebral glutamate in situ as detected by ^{1}H/^{13}C n.m.r. Biochem. J. 298 (Pt 1), 121–127.

Kegeles, L.S., Mao, X., Stanford, A.D., Girgis, R., Ojeil, N., Xu, X., Gil, R., Slifstein, M., Abi-Dargham, A., Lisanby, S.H., Shungu, D.C., 2012. Elevated prefrontal cortex gamma-aminobutyric acid and glutamate-glutamine levels in schizophrenia measured in vivo with proton magnetic resonance spectroscopy. Arch. Gen. Psychiatry 69, 449–459.

Lewis, D.A., Hashimoto, T., Volk, D.W., 2005. Cortical inhibitory neurons and schizophrenia. Nat. Rev. Neurosci. 6, 312–324.

Lisman, J.E., Coyle, J.T., Green, R.W., Javitt, D.C., Benes, F.M., Heckers, S., Grace, A.A., 2008. Circuit-based framework for understanding neurotransmitter and risk gene interactions in schizophrenia. Trends Neurosci. 31, 234–242.

Magistretti, P.J., Pellerin, L., Rothman, D.L., Shulman, R.G., 1999. Energy on demand. Science 283, 496–497.

Mangia, S., Tkac, I., Gruetter, R., Van de Moortele, P.F., Maraviglia, B., Ugurbil, K., 2007. Sustained neuronal activation raises oxidative metabolism to a new steady-state level: evidence from ^{1}H NMR spectroscopy in the human visual cortex. J. Cereb. Blood Flow Metab. 27, 1055–1063.

Mann, E.O., Mody, I., 2010. Control of hippocampal gamma oscillation frequency by tonic inhibition and excitation of interneurons. Nat. Neurosci. 13, 205–212.

Martens, U., Gruber, T., 2012. Sharpening and formation: two distinct neuronal mechanisms of repetition priming. Eur. J. Neurosci. 36, 2989–2995.

Martinovic, J., Busch, N.A., 2011. High frequency oscillations as a correlate of visual perception. Int. J. Psychophysiol. 79, 32–38.

Mayer, D., Spielman, D.M., 2005. Detection of glutamate in the human brain at 3 T using optimized constant time point resolved spectroscopy. Magn. Reson. Med. 54, 439–442.

Morris, R.G., 1989. Synaptic plasticity and learning: selective impairment of learning in rats and blockade of long-term potentiation in vivo by the N-methyl-D-aspartate receptor antagonist AP5. J. Neurosci. 9, 3040–3057.

Mullins, P.G., Rowland, L.M., Jung, R.E., Sibbitt Jr., W.L., 2005. A novel technique to study the brain's response to pain: proton magnetic resonance spectroscopy. Neuroimage 26, 642–646.

Mullins, P.G., Chen, H., Xu, J., Caprihan, A., Gasparovic, C., 2008. Comparative reliability of proton spectroscopy techniques designed to improve detection of J-coupled metabolites. Magn. Reson. Med. 60, 964–969.

Muthukumaraswamy, S.D., Edden, R.A., Jones, D.K., Swettenham, J.B., Singh, K.D., 2009. Resting GABA concentration predicts peak gamma frequency and fMRI amplitude in response to visual stimulation in humans. Proc. Natl. Acad. Sci. U. S. A. 106, 8356–8361.

Myme, C.I., Sugino, K., Turrigiano, G.G., Nelson, S.B., 2003. The NMDA-to-AMPA ratio at synapses onto layer 2/3 pyramidal neurons is conserved across prefrontal and visual cortices. J. Neurophysiol. 90, 771–779.

Naressi, A., Couturier, C., Devos, J.M., Janssen, M., Mangeat, C., de Beer, R., Graveron-Demilly, D., 2001. Java-based graphical user interface for the MRUI quantitation package. MAGMA 12, 141–152.

Nishitani, N., 2003. Dynamics of cognitive processing in the human hippocampus by neuromagnetic and neurochemical assessments. Neuroimage 20, 561–571.

Oppermann, F., Hassler, U., Jescheniak, J.D., Gruber, T., 2012. The rapid extraction of gist-early neural correlates of high-level visual processing. J. Cogn. Neurosci. 24, 521–529.

Picton, T.W., Bentin, S., Berg, P., Donchin, E., Hillyard, S., et al., 2000. Guidelines for using human event-related potentials to study cognition: recording standards and publication criteria. Psychophysiology 37 (2), 127–152.

Rao, V.R., Finkbeiner, S., 2007. NMDA and AMPA receptors: old channels, new tricks. Trends Neurosci. 30, 284–291.

Rodriguez, R., Kallenbach, U., Singer, W., Munk, M.H., 2004. Short- and long-term effects of cholinergic modulation on gamma oscillations and response synchronization in the visual cortex. J. Neurosci. 24, 10369–10378.

Ronnqvist, K.C., McAllister, C.J., Woodhall, G.L., Stanford, I.M., Hall, S.D., 2013. A multimodal perspective on the composition of cortical oscillations. Front. Hum. Neurosci. 7, 132.

Rothman, D.L., Sibson, N.R., Hyder, F., Shen, J., Behar, K.L., Shulman, R.G., 1999. In vivo nuclear magnetic resonance spectroscopy studies of the relationship between the glutamate-glutamine neurotransmitter cycle and functional neuroenergetics. Philos. Trans. R. Soc. Lond. B Biol. Sci. 354, 1165–1177.

Roye, A., Schroger, E., Jacobsen, T., Gruber, T., 2010. Is my mobile ringing? Evidence for rapid processing of a personally significant sound in humans. J. Neurosci. 30, 7310–7313.

Schubert, F., Gallinat, J., Seifert, F., Rinneberg, H., 2004. Glutamate concentrations in human brain using single voxel proton magnetic resonance spectroscopy at 3 tesla. Neuroimage 21, 1762–1771.

Shen, J., 2013. Modeling the glutamate-glutamine neurotransmitter cycle. Front. Neuroenergetics 5, 1.

Singer, W., 1999. Neuronal synchrony: a versatile code for the definition of relations? Neuron 24 (49–65), 111–125.

Stephan, K.E., Baldeweg, T., Friston, K.J., 2006. Synaptic plasticity and dysconnection in schizophrenia. Biol. Psychiatry 59, 929–939.
Tallon-Baudry, C., Bertrand, O., 1999. Oscillatory gamma activity in humans and its role in object representation. Trends Cogn. Sci. 3, 151–162.
Valette, J., Guillermier, M., Besret, L., Boumezbeur, F., Hantraye, P., Lebon, V., 2005. Optimized diffusion-weighted spectroscopy for measuring brain glutamate apparent diffusion coefficient on a whole-body MR system. NMR Biomed. 18, 527–533.
Wespatat, V., Tennigkeit, F., Singer, W., 2004. Phase sensitivity of synaptic modifications in oscillating cells of rat visual cortex. J. Neurosci. 24, 9067–9075.
Whittington, M.A., Traub, R.D., Jefferys, J.G., 1995. Synchronized oscillations in interneuron networks driven by metabotropic glutamate receptor activation. Nature 373, 612–615.
Wiggs, C.L., Martin, A., 1998. Properties and mechanisms of perceptual priming. Curr. Opin. Neurobiol. 8, 227–233.
Womelsdorf, T., Fries, P., Mitra, P.P., Desimone, R., 2006. Gamma-band synchronization in visual cortex predicts speed of change detection. Nature 439, 733–736.
Yuval-Greenberg, S., Tomer, O., Keren, A.S., Nelken, I., Deouell, L.Y., 2008. Transient induced gamma-band response in EEG as a manifestation of miniature saccades. Neuron 58, 429–441.